MethodsX 8 (2021) 101291

Contents lists available at ScienceDirect

MethodsX

journal homepage: www.elsevier.com/locate/mex

Method Article

# Updating a Paleogene magnetobiochronological time scale through graphical integration

Gabriela J. Arreguín-Rodríguez[a,b,*], Carlos A. Trasviña-Moreno[c], Ellen Thomas[d,e], Laia Alegret[f,g]

[a] Centro Interdisciplinario de Ciencias Marinas del Instituto Politécnico Nacional, La Paz, Baja California Sur, Mexico
[b] Facultad de Ciencias Marinas, Universidad Autónoma de Baja California, Ensenada, Baja California 22860, Mexico
[c] HOWLab – Human Openware Research Lab, Instituto de Investigación en Ingeniería de Aragón, Universidad de Zaragoza, Spain
[d] Department of Earth and Planetary Sciences, Yale University, New Haven, CT, United States
[e] Department of Earth and Environmental Sciences, Wesleyan University, Middletown, CT, USA
[f] Departamento de Ciencias de la Tierra, Universidad de Zaragoza, Pedro Cerbuna 12, Zaragoza 50009, Spain
[g] Instituto Universitario de Ciencias Ambientales, Universidad de Zaragoza, Zaragoza, Spain

ABSTRACT

All studies focused on the evaluation of paleoecological variability over geological time must be linked to a specific age or time interval, which can be defined using different time scales (biostratigraphic, chronostratigraphic, geochronological or orbital). Therefore, integrated time scales are essential to allow comparisons of data from different locations and/or to assess evolutionary and other events through time. Here we use a new method to update a Paleogene magnetobiochronological time scale, with the following contributions:

- The update of the Paleogene magnetobiochronological scale was made by graphical correlation with new age models and adding calcareous nannoplankton and planktonic foraminiferal biozones from different authors.
- An excel file structure was proposed to plot any kind of data in MATLAB software, as long as they are associated with some of the scales shown in our updated version of Paleogene magnetobiochronology.
- The excel file structure facilitates the analysis of long-term trends of taxonomic groups throughout the Paleogene, and of their evolution in a period characterized by intense climate variability.



DOI of original article: 10.1016/j.gloplacha.2020.103372

* Corresponding author at: Facultad de Ciencias Marinas, Universidad Autónoma de Baja California, Ensenada, Baja California 22860, Mexico.

*E-mail address:* arreguing@uabc.edu.mx (G.J. Arreguín-Rodríguez).

https://doi.org/10.1016/j.mex.2021.101291

ARTICLE INFO
*Method name:* Graphical update of a magnetobiochronologic/orbital time scale.
*Keywords:* Paleogene, Biostratigraphy, Chronostratigraphy, Geochronology, Age model, Time scale
*Article history:* Received 3 December 2020; Accepted 24 February 2021; Available online 28 February 2021

Specifications table

| | |
|---|---|
| Subject Area: | Earth and Planetary Sciences |
| More specific subject area: | *Paleoecology.* |
| Method name: | *Graphical update of a magnetobiochronologic/orbital time scale.* |
| Name and reference of original method: | *Integrated magnetobiochronologic/orbital time scale*<br>*[1] Berggren, W., and Pearson, P. A revised tropical to subtropical Paleogene planktonic foraminiferal zonation. Journal of Foraminiferal Research, 35 (2005), pp. 279–298.* |
| Resource availability: | *Software: MATLAB, Adobe Illustrator, Microsoft Excel.*<br>*Supplementary material is available within this article.* |

## Method details

Step 1. We digitized the Paleocene, Eocene and Oligocene chronostratigraphical and biostratigraphical (including calcareous nannoplankton [2–5] and planktonic foraminifera biozones [1, 6]) time scales as integrated by Berggren and Pearson [1]. In Berggren and Pearson [1], these scales are shown by epoch, and only some chrons and biozones of the contiguous epochs are indicated in each case. We thus joined them in a single plot by overlapping the contiguous biozones.

Step 2. Other calcareous nannoplankton [7] and planktonic foraminifera [8–10] biozones were added to the constructed plot. Such additions consisted of the digitization of the new biozones together with a reference biozonation that allowed us to place them correctly into the plot.

Step 3. Since the epoch plots were separated in Berggren and Pearson [1], different vertical scales were used in each plot. In order to standardize the vertical scale, we looked for the numerical age of key chrons, i.e., the first and last complete chrons of each epoch, as well as the chrons within the boundary intervals between epochs (Paleocene-Eocene and Eocene-Oligocene; Table 1). The age of these chrons was obtained from the ODSN website [11], which provides numerical ages according to different timescale models for magnetic events. Here, we followed the age model of Gradstein et al. [12].

The length of intervals and the age of chrons in Table 1 were used to construct the numerical age scales for each interval in MATLAB [13]. These scales were employed to obtain the equivalence of a million years in millimetres to achieve a greater precision, measuring graphically in Adobe Illustrator [14] (Table 2). Millimetres were not used in MATLAB since these are not a valid measuring unit. Equivalence data were required to develop a standard vertical scale.

**Table 1**
Numerical age [12] of chrons used for the standardization of vertical scale.

| Interval | Chron | Ma (chron top) | Length of intervals (inches) |
|---|---|---|---|
| Oligocene | C6Cn3n | 23.233 | 1.97 |
| | C13r | 33.705 | |
| Eocene - Oligocene boundary | C13r | 33.705 | 0.23 |
| | C15n | 34.999 | |
| Eocene | C15n | 34.999 | 3.8 |
| | C24r | 53.983 | |
| Paleocene - Eocene boundary | C24r | 53.983 | 0.52 |
| | C25n | 57.101 | |
| Paleocene - upper Cretaceous | C25n | 57.101 | 2.4 |
| | C30r | 68.196 | |

**Table 2**
Length of 1 myr per interval.

| Interval | Length of 1 myr (mm) |
|---|---|
| Oligocene | 4.790 |
| Eocene - Oligocene boundary | 4.440 |
| Eocene | 5.080 |
| Paleocene - Eocene boundary | 4.250 |
| Paleocene - upper Cretaceous | 5.495 |

**Table 3**
Re-scaling factors for the standardization of the vertical scale.

| Interval | Pre-adjustment re-scaling factor | Final re-scaling factor |
|---|---|---|
| Eocene - Oligocene boundary | 1.0788 | 1.0799 |
| Eocene | 0.9429 | 0.9429 |
| Paleocene - Eocene boundary | 1.1270 | 1.1278 |
| Paleocene - Upper Cretaceous | 0.8717 | 0.8713 |

For the standardization of the vertical scales, re-scaling factors were calculated (Table 3) using the Oligocene interval as reference. This was achieved by dividing the length of 1 myr from the Oligocene (4.790 mm), among the length of each of the other intervals (Table 2). Minor graphical adjustments were required for a proper fit of the re-scaled numerical age axis ($<0.001$).

Step 4. Following the results in Table 3, the re-scaling process of numerical age, chronostratigraphical and biostratigraphical scales was done in Adobe Illustrator, and a single plot for the entire Paleogene was obtained.

Step 5. In order to validate the obtained Paleogene magnetobiochronological scale, carbon and oxygen isotope data from Zachos et al. [15] was plotted using the Gradstein et al. [12] age model. Well-known global stable isotope shifts that characterize the boundaries of some epochs allowed us to validate the Paleogene scale. At the Paleocene-Eocene boundary, a large amount of isotopically light carbon was added into the ocean-atmosphere system causing a unique negative excursion of $\delta^{13}C$ values [16]; at the Eocene-Oligocene boundary, a notable increase in $\delta^{18}O$ values is recorded reflecting the beginning of Oligocene glaciation [17]. We observed a perfect fit between isotope curves and chronostratigraphic and biostratigraphic schemes. However, the negative excursion of $\delta^{13}C$ values did not coincide with the Paleocene-Eocene boundary.

Step 6. To solve this, we replaced $\delta^{13}C$ and $\delta^{18}O$ data from Zachos et al. [15] by a stable isotope record based on an updated age model [18], which extends from the late Maastrichtian up to the early Eocene. In spite of this, curves still did not fit properly at the Paleocene-Eocene boundary, thus a second re-scaling was applied. For this re-scaling, we considered that the Cretaceous-Paleogene boundary and the Paleocene-Eocene boundary are anchored at 66.0225 [19] and 55.93 Ma [20] respectively, following the specifications in [18]. This implies that the length of the Eocene had to be reduced by a factor of 0.9698, whereas the Paleocene had to be expanded by a factor of 1.1075. After this adjustment, the re-scaling of the Paleogene magnetobiochronological scale was validated (Fig. 1).

Step 7. The validated magnetobiochronological plot was used to obtain pixel data corresponding to the limits of the biozones of interest. This was achieved using the imtool function of MATLAB, which displays a grey scale image of the selected file in the image viewer app. Importantly, the file used in this step must be an RGB TIF file with a resolution of 1500 dpi, and must not include any headers in the figure (Supplementary Fig. 1). The Y axis coordinate (pixel value) was extracted for the top and bottom limits of each of the selected biozones, using the information displayed in the image viewer app. From such data, the average pixel value of each biozone was calculated (Supplementary Table 1).

Step 8. In order to plot any data against the magnetobiochronological scale, an excel file structure was designed to link the paleoecological data (e.g., abundance of specific taxa, diversity index, etc.) to the average Y pixel values of the corresponding biozone (Fig. 2).

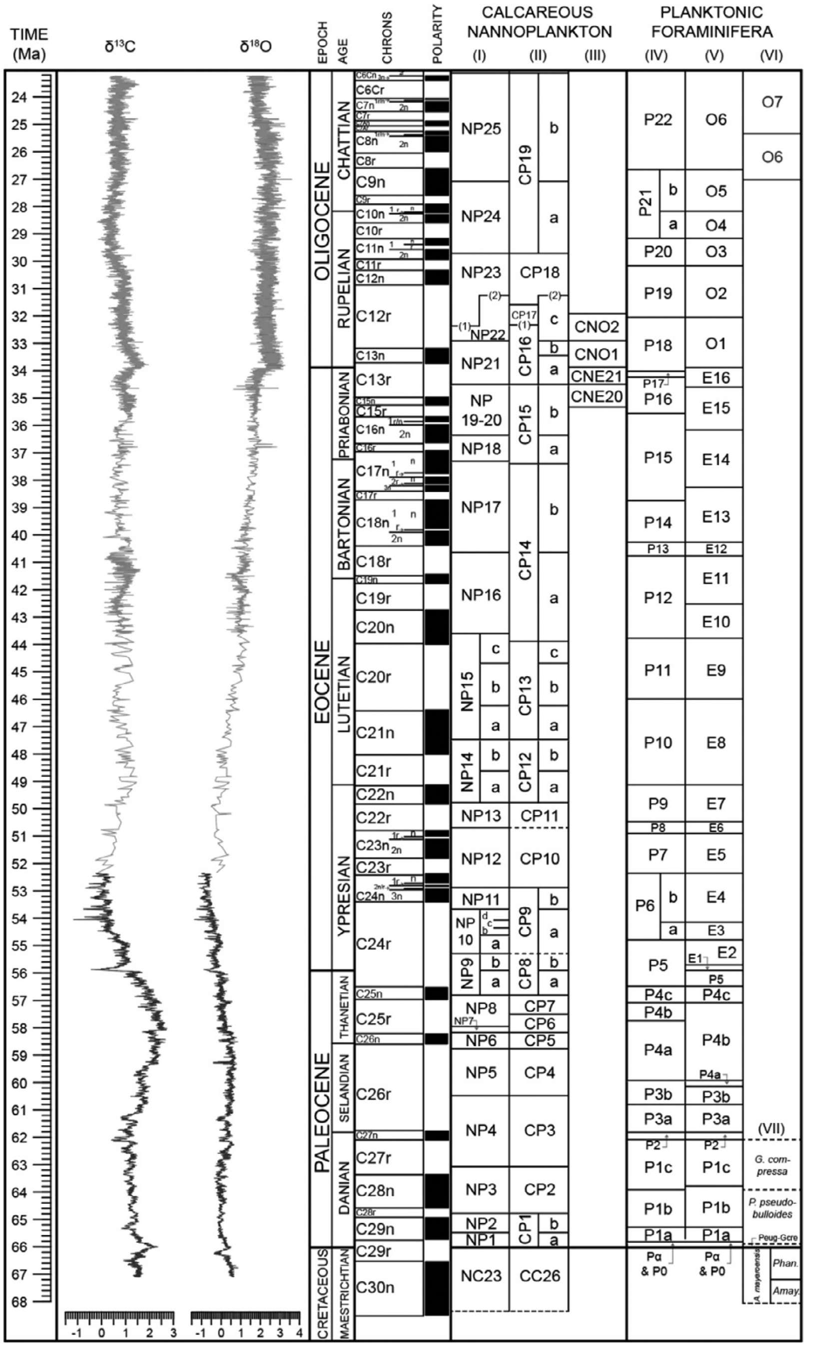


**Fig. 1.** Validated Paleogene magnetobiochronological scale. Benthic foraminifera $\delta^{13}C$ and $\delta^{18}O$ data from Zachos et al. [15] and Barnet et al. [18] (see references therein [18]) are plotted against timescale using age model from Gradstein et al. [12] and Barnet et al. [18]. Calcareous nannoplankton biozones: I [2], II [3–5], and III [7]; planktonic foraminiferal biozones: IV [6], V [1], VI [8], VII [9, 10].

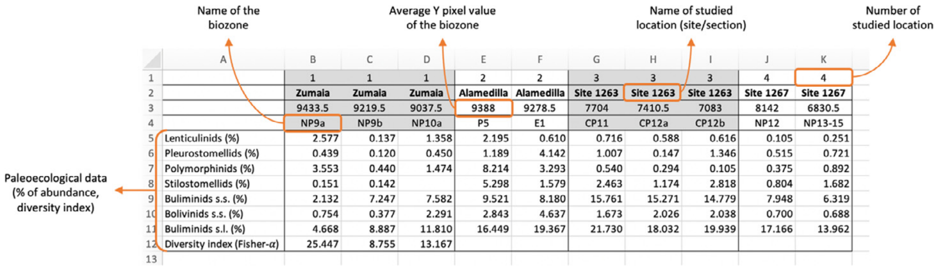


| | A | B | C | D | E | F | G | H | I | J | K |
|---|---|---|---|---|---|---|---|---|---|---|---|
| 1 | | 1 | 1 | 1 | 2 | 2 | 3 | 3 | 3 | 4 | 4 |
| 2 | | Zumaia | Zumaia | Zumaia | Alamedilla | Alamedilla | Site 1263 | Site 1263 | Site 1263 | Site 1267 | Site 1267 |
| 3 | | 9433.5 | 9219.5 | 9037.5 | 9388 | 9278.5 | 7704 | 7410.5 | 7083 | 8142 | 6830.5 |
| 4 | | NP9a | NP9b | NP10a | P5 | E1 | CP11 | CP12a | CP12b | NP12 | NP13-15 |
| 5 | Lenticulinids (%) | 2.577 | 0.137 | 1.358 | 2.195 | 0.610 | 0.716 | 0.588 | 0.616 | 0.105 | 0.251 |
| 6 | Pleurostomellids (%) | 0.439 | 0.120 | 0.450 | 1.189 | 4.142 | 1.007 | 0.147 | 1.346 | 0.515 | 0.721 |
| 7 | Polymorphinids (%) | 3.553 | 0.440 | 1.474 | 8.214 | 3.293 | 0.540 | 0.294 | 0.105 | 0.375 | 0.892 |
| 8 | Stilostomellids (%) | 0.151 | 0.142 | | 5.298 | 1.579 | 2.463 | 1.174 | 2.818 | 0.804 | 1.682 |
| 9 | Buliminids s.s. (%) | 2.132 | 7.247 | 7.582 | 9.521 | 8.180 | 15.761 | 15.271 | 14.779 | 7.948 | 6.319 |
| 10 | Bolivinids s.s. (%) | 0.754 | 0.377 | 2.291 | 2.843 | 4.637 | 1.673 | 2.026 | 2.038 | 0.700 | 0.688 |
| 11 | Buliminids s.l. (%) | 4.668 | 8.887 | 11.810 | 16.449 | 19.367 | 21.730 | 18.032 | 19.939 | 17.166 | 13.962 |
| 12 | Diversity index (Fisher-$\alpha$) | 25.447 | 8.755 | 13.167 | | | | | | | |
| 13 | | | | | | | | | | | |

**Fig. 2.** Example of key elements and required set-up of the excel file (Supplementary Table 2) used to plot paleoecological data against the updated Paleogene magnetobiochronological scale.

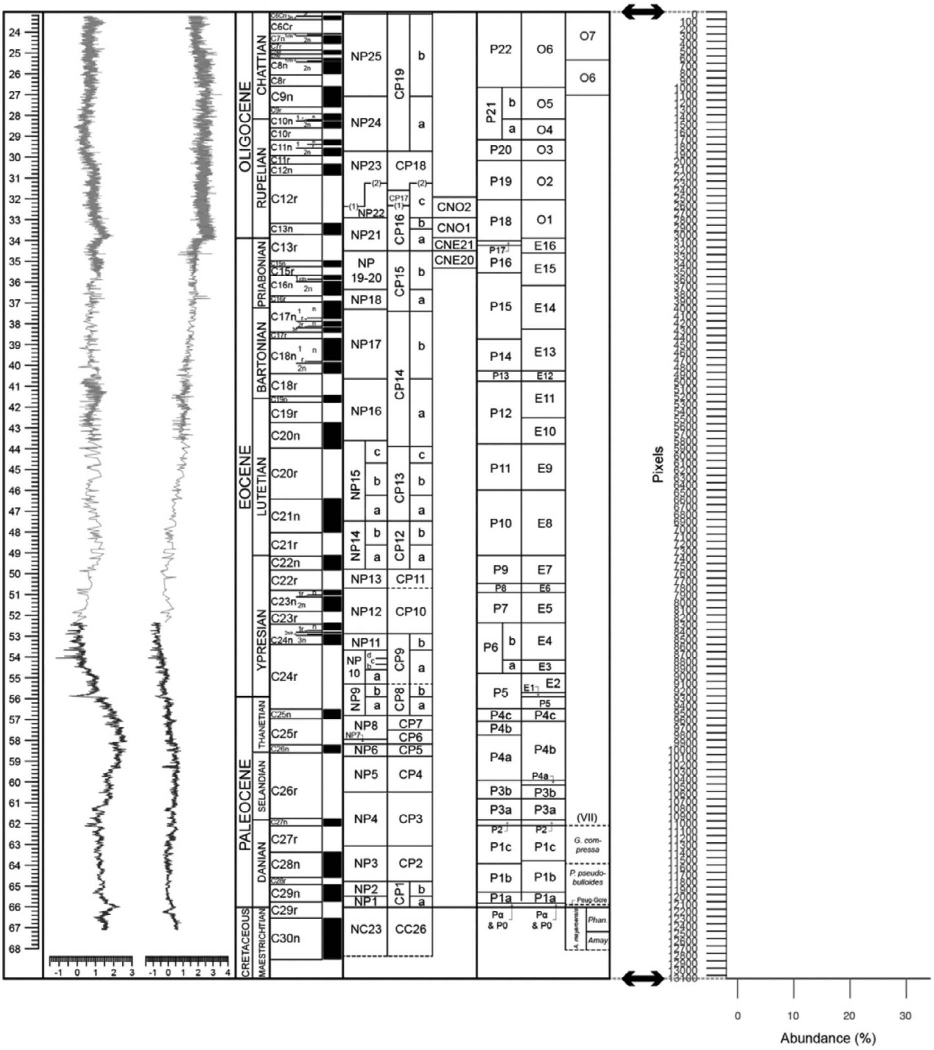


**Fig. 3.** Comparison between the Y axis coordinate plot developed in MATLAB and the updated Paleogene magnetobiochronological scale.

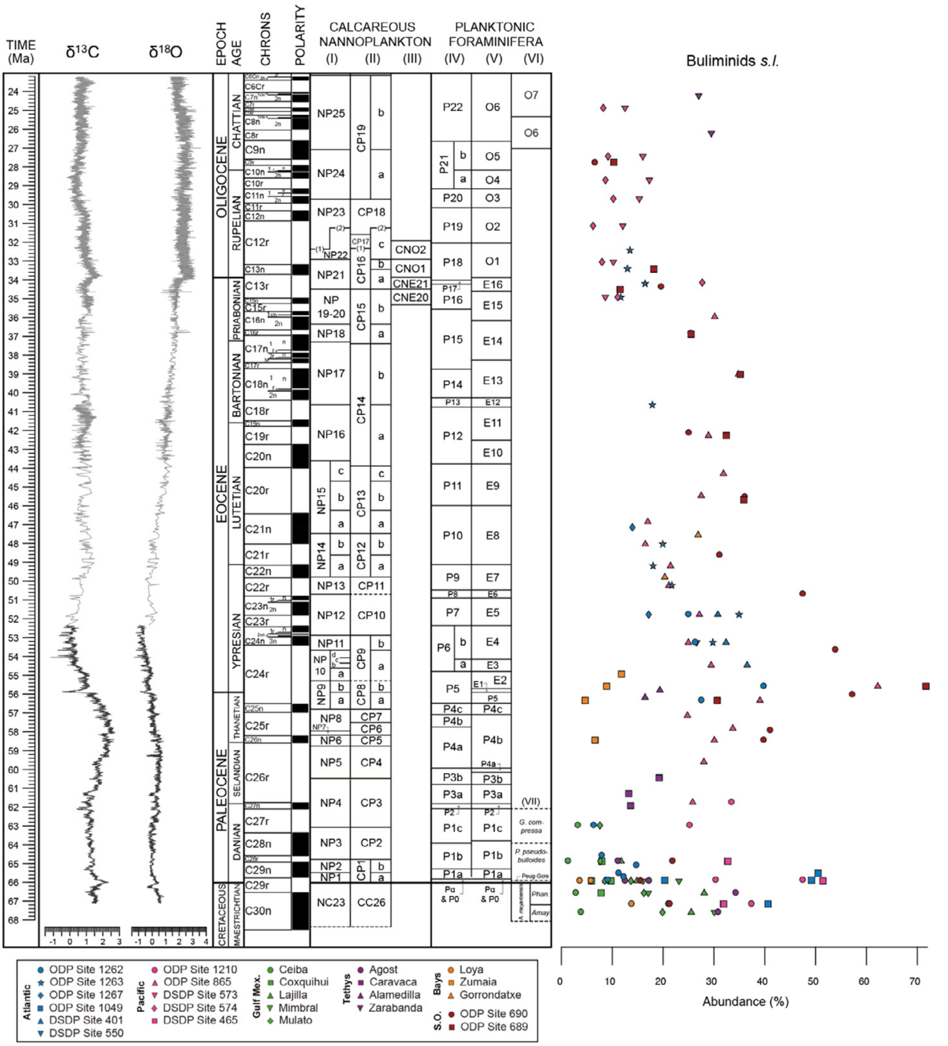


**Fig. 4.** Implementation of the method for plotting paleoecological data such as the relative abundance of a group of benthic foraminifera (buliminids *sensu lato, s.l.*) against the updated Paleogene magnetobiochronological scale. Benthic foraminifera $\delta^{13}$C and $\delta^{18}$O data from Zachos et al. [15] and Barnet et al. [18] (see references therein [18]) are plotted against timescale using the age model from Gradstein et al. [12] and Barnet et al. [18]. Calcareous nannoplankton biozones: I [2], II [3–5], and III [7]; planktonic foraminiferal biozones: IV [6], V [1], VI [8], VII [9, 10].

Step 9. Once the paleoecological data was included in the excel file, the data was plotted in MATLAB using the average Y pixel value (Supplementary Source Code). The resulting graph has the same vertical size as the file used in the image viewer app (Fig. 3). The horizontal axis displays the paleoecological data (e.g., relative abundance of taxa, diversity index, etc.), and the vertical axis shows the pixel scale, with values in descending order. The vertical axis must be displayed on this scale and in this format (descending values) because the MATLAB image viewer app uses a descending coordinate system, with the origin coordinates in the upper-left corner. Fig. 4 shows an example of the plotted data as compared with the magnetobiochronological scale. The paleoecological data displayed in Fig. 4 were extracted from the compilation of benthic foraminiferal quantitative data, in order to analyze the spatial/temporal variability of these organisms through the Paleogene [21].

## Declaration of Competing Interest

The authors declare that they have no known competing financial interests or personal relationships that could have appeared to influence the work reported in this paper.

## Acknowledgments

This work was supported by the Spanish Ministry of Economy and Competitiveness and FEDER funds (CGL2017–84693-R and PID2019–105537RB-I00), the Government of Aragon (Reference Group E33_17R, co-financed with FEDER 2014–2020 "Building Europe from Aragon"), by SEP-CONACyT (221705) and partially by NSF (OCE 1536611). This study includes data from samples provided by the Integrated Ocean Drilling Program (IODP).

## Supplementary materials

Supplementary material associated with this article can be found, in the online version, at doi:10.1016/j.mex.2021.101291.

## References

[1] W. Berggren, P. Pearson, A revised tropical to subtropical Paleogene planktonic foraminiferal zonation, J. Foraminifer. Res. 35 (2005) 279–298.
[2] E. Martini, Standard Tertiary and Quarternary Calcareous Nannoplankton Zonation, in: A. Farinacci (Ed.), Proceedings of the 2nd Planktonic Conference, Rome, Italy, Tecnoscienza, 1971, pp. 739–785.
[3] D. Bukry, et al., Low-latitude biostratigraphic zonation, in: NT Edgar, JB Saunders, et al. (Eds.), Initial Reports of the Deep Sea Drilling Project 15, U.S. Government Printing Office, Washington, 1973, pp. 685–703.
[4] D. Bukry, et al., Coccolith and silicoflagellate stratigraphy, northwestern Pacific Ocean, Deep Sea Drilling Project Leg 32, in: RL Larson, R Moberly, et al. (Eds.), Initial Reports of the Deep Sea Drilling Project 32, U.S. Government Printing Office, Washington, 1975, pp. 677–701.
[5] H. Okada, D Bukry, Supplementary modification and introduction of code numbers to the low-latitude coccolith biostratigraphic zonation (Bukry, 1973; 1975), Mar. Micropaleontol. 5 (1980) 321–325.
[6] W.A. Berggren, D.V. Kent, C.C. Swisher, M.P. Aubry, A revised Cenozoic geochronology and chronostratigraphy, in: W.A. Berggren, D.V. Kent, C.C.III Swisher, M.P. Aubry, J. Hardenbol (Eds.), Geochronology, Time Scales and Global Stratigraphic Correlation, SEPM (Society for Sedimentary Geology) Special Publication, USA, 1995, pp. 129–212. 54.
[7] C. Agnini, E. Fornaciari, I. Raffi, R. Catanzariti, H. Pälike, J. Backman, D. Rio, Biozonation and biochronology of Paleogene calcareous nannofossils from low and middle latitudes, Newsl. Strat. 47 (2) (2014) 131–181.
[8] B. Wade, P.N. Pearson, W.A. Berggren, H. Pälike, Review and revision of Cenozoic tropical planktonic foraminiferal biostratigraphy and calibration to the geomagnetic polarity and astronomical time scale, Earth-Sci. Rev. 104 (2011) 111–142.
[9] E. Molina, I. Arenillas, J.A. Arz, The Cretaceous-Tertiary boundary mass extinction in planktic foraminifera at Agost, Spain, Revue de Micropaléontogie 39 (1996) 225–243.
[10] I. Arenillas, J.A. Arz, E. Molina, A new high-resolution planktic foraminiferal zonation and subzonation for the lower Danian, Lethaia 37 (2004) 79–95.
[11] Ocean Drilling Stratigraphic Network. Available online: https://www.odsn.de/odsn/services/conv_ts/conv_ts.html (accessed on October 17, 2020).
[12] F.M. Gradstein, J.G. Ogg, M.D. Schmitz, G.M. Ogg, The Geologic Time Scale 2012, Elsevier, Amsterdam, Netherlands, 2012.
[13] MathWorks MATLAB. Available online: https://www.mathworks.com/products/matlab.html (accessed on October 17, 2020).
[14] Adobe Illustrator. Available online: https://www.adobe.com/mx/products/illustrator.html (accessed on October 17, 2020).
[15] J.C. Zachos, G.R. Dickens, R.E. Zeebe, An early Cenozoic perspective on greenhouse warming and carbon-cycle dynamics, Nature 451 (2008) 279–283.
[16] G.R. Dickens, M.M. Castillo, J.C.G. Walker, A blast of gas in the latest Paleocene: simulating first order effects of massive dissociation of oceanic methane hydrate, Geology 25 (1997) 259–262.
[17] J. Zachos, M. Pagani, L. Sloan, E. Thomas, K. Billups, Trends, rhythms, and aberrations in global climate 65 Ma to present, Science 292 (2001) 686–693.
[18] J.S.K Barnet, K. Littler, T. Westerhold, D. Kroon, M.J. Leng, I. Bailey, U. Röhl, J Zachos, A high-fidelity benthic stable isotope record of Late Cretaceous-early Eocene climate change and carbon-cycling, Paleoceanography and Paleoclimatology 34 (2019) 672–691.
[19] J. Dinarés-Turell, T. Westerhold, V. Pujalte, U. Röhl, D. Kroon, Astronomical calibration of the Danian stage (early Paleocene) revisited: settling chronologies of sedimentary records across the Atlantic and Pacific oceans, Earth Planet. Sci. Lett. 405 (2014) 119–131.

[20] T. Westerhold, U. Röhl, J. Laskar, I. Raffi, J. Bowles, L.J. Lourens, J.C. Zachos, On the duration of magnetochrons C24r and C25n and the timing of early Eocene global warming events: implications from the ocean drilling program leg 208 walvis ridge depth transect, Paleoceanography 22 (2007) PA2201.

[21] L. Alegret, G.J. Arreguín-Rodríguez, C.A. Trasviña-Moreno, E. Thomas, Turnover and stability in the deep sea: benthic foraminifera as tracers of Paleogene global change, Glob. Planet. Change (2021), doi:10.1016/j.gloplacha.2020.103372.